is interpreted to indicate a stronger monsoon (*40*). Morrill *et al.* summarized evidence for an abrupt monsoon shift around 1300 that is heterogeneous in geographical extent (*41*). The centuries-long increase in the southwest monsoon between 1000 and 1500 coincides with a wet phase in India, as observed in the speleothem data from central and eastern regions of the country (*42*). Although these studies support the major trends in our record, more data are needed to test our hypothesized changes in monsoon strength over the past 1000 years, particularly over Tibet and regions of India strongly affected by the southwest monsoon.

References

1. W. L. Prell, D. Murray, S. C. Clemens, D. M. Anderson, in *Synthesis of Results from Scientific Drilling in the Indian Ocean*, R. A. Duncan *et al.*, Eds. (Geophysical Monograph 70, American Geophysical Union, Washington, DC, 1992), pp. 447–469.
2. Z. T. Guo *et al.*, *Nature* **416**, 159 (2002).
3. M. A. Altabet, R. Francoise, D. M. Murray, W. L. Prell, *Nature* **373**, 506 (1995).
4. J. E. Kutzbach, F. A. Street-Perrott, *Nature* **317**, 130 (1985).
5. S. C. Clemens, W. L. Prell, D. W. Murray, G. Shimmield, G. Weedon, *Science* **353**, 720 (1991).
6. S. C. Clemens, D. W. Murray, W. L. Prell, *Science* **274**, 943 (1996).
7. D. M. Anderson, W. L. Prell, *Paleoceanography* **8**, 193 (1993).
8. G. J. Reichart, L. J. Lourens, W. J. Zachariasse, *Paleoceanography* **13**, 607 (1998).
9. P. D. Naidu, B. J. Malmgren, *Paleoceanography* **11**, 129 (1996).
10. J. T. Overpeck, D. M. Anderson, S. Trumbore, W. L. Prell, *Clim. Dyn.* **12**, 213 (1996).
11. COHMAP Project Members, *Science* **241**, 1043 (1988).
12. F. Sirocko *et al.*, *Nature* **364**, 322 (1993).
13. M. A. Altabet, M. J. Higginson, D. W. Murray, *Nature* **415**, 159 (2002).
14. F. Sirocko, D. Garbe-Schonberg, A. McIntyre, B. Molfino, *Science* **272**, 526 (1996).
15. G. A. Meehl, *Science* **266**, 263 (1994).
16. T. P. Barnett, L. Dumenil, U. Schlese, E. Roeckner, M. Latif, *J. Atmos. Sci.* **46**, 661 (1989).
17. L. Wang *et al.*, *Geophys. Res. Lett.* **26**, 2889 (1999).
18. D. M. Anderson, *Paleoceanography* **16**, 352 (2001).
19. T. J. Goreau, *Nature* **287**, 620 (1980).
20. W. L. Prell, in *Climate Processes and Climate Sensitivity*, J. E. Hansen, T. Takahashi, Eds. (American Geophysical Union, Washington, DC, 1984), pp. 48–57.
21. W. B. Curry, D. R. Ostermann, M. V. S. Guptha, V. Ittekkot, in *Upwelling Systems: Evolution Since the Early Miocene*, C. P. Summerhayes, W. L. Prell, K. C. Emeis, Eds. (Geological Society, London, 1992), pp. 93–106.
22. D. E. Black *et al.*, *Science* **286**, 1709 (1999).
23. M. Stuiver, P. J. Reimer, *Radiocarbon* **35**, 15 (1993).
24. M. Stuiver, T. F. Braziunas, *Radiocarbon* **35**, 137 (1993).
25. D. M. Anderson, thesis, Brown University (1991).
26. S. Huang, H. N. Pollack, P.-Y. Shen, *Nature* **403**, 756 (2000).
27. W. L. Prell, in *Milankovitch and Climate, Part 1*, A. L. Berger *et al.*, Eds. (American Geophysical Union, Washington, DC, 1984), pp. 48–57.
28. M. E. Mann, R. S. Bradley, M. K. Hughes, *Geophys. Res. Lett.* **26**, 759 (1999).
29. R. J. Slutz *et al.*, *Comprehensive Ocean-Atmosphere Data Set; Release 1* (Climate Research Program, Boulder, CO, 1985).
30. B. Parthasarathy, A. A. Munot, D. R. Kothawale, *Theor. Appl. Climatol.* **49**, 217 (1994).
31. K. Y. Vinnikov, A. Robock, *Geophys. Res. Lett.* **29**, 1029 (2002).
32. I. Subbaramayya, C. V. Naidu, *Int. J. Climatol.* **12**, 597 (1992).
33. D. A. Mooley, G. B. Pant, in *Climate and History*, T. M. L. Wigley, M. S. Ingram, G. Farmer, Eds. (Cambridge Univ. Press, Cambridge, 1981), pp. 465–478.
34. M. Sankar-Rao, K. M. Lau, S. Yang, *Int. J. Climatol.* **16**, 605 (1996).
35. S. C. Porter, A. Zhisheng, *Nature* **375**, 305 (1995).
36. W. J. Burroughs, *Does the Weather Really Matter? The Social Implications of Climatic Change* (Cambridge Univ. Press, Cambridge, 1997).
37. P. D. Jones, R. S. Bradley, in *Climate Since A.D. 1500*, R. S. Bradley, P. D. Jones, Eds. (Routledge, New York, 1992), pp. 649–665.
38. G. C. Jacoby, R. D. D'Arrigo, T. Davaajamts, *Science* **273**, 771 (1996).
39. C. Sharma, M. S. Chauhan, *J. Paleontol. Soc. India* **46**, 51 (2001).
40. G. Ren, *Geophys. Res. Lett.* **25**, 1931 (1998).
41. C. Morrill, J. T. Overpeck, J. E. Cole, in preparation.
42. M. G. Yadava, R. Ramesh, *J. Sci. Industr. Res.* **58**, 339 (1999).

Supporting Online Material

www.sciencemag.org/cgi/content/full/297/5581/596/DC1
Supporting Text
Figs. S1 and S2
Tables S1 and S2

15 April 2002; accepted 6 June 2002

Fork Reversal and ssDNA Accumulation at Stalled Replication Forks Owing to Checkpoint Defects

José M. Sogo,[1]* Massimo Lopes,[2]* Marco Foiani[2]†

Checkpoint-mediated control of replicating chromosomes is essential for preventing cancer. In yeast, Rad53 kinase protects stalled replication forks from pathological rearrangements. To characterize the mechanisms controlling fork integrity, we analyzed replication intermediates formed in response to replication blocks using electron microscopy. At the forks, wild-type cells accumulate short single-stranded regions, which likely causes checkpoint activation, whereas *rad53* mutants exhibit extensive single-stranded gaps and hemi-replicated intermediates, consistent with a lagging-strand synthesis defect. Further, *rad53* cells accumulate Holliday junctions through fork reversal. We speculate that, in checkpoint mutants, abnormal replication intermediates begin to form because of uncoordinated replication and are further processed by unscheduled recombination pathways, causing genome instability.

Chromosome integrity during DNA replication is essential for preventing genome rearrangements and cancer (*1–3*). When replication pauses, the stability of stalled forks is controlled by the checkpoint (*4*, *5*), which, in *Saccharomyces*, requires Rad53 kinase activation (*6*). Active Rad53 somehow prevents accumulation of abnormal intermediates allowing the forks to restart DNA synthesis (*4*, *7*, *8*). Hydroxyurea-treated *rad53* cells accumulate DNA structures that impede replication resumption when the inhibitor is removed (*4*).

In vivo psoralen cross-linking and electron microscopy (*9*) were used to analyze these intermediates. Samples from hydroxyurea-treated wild-type and *rad53* cells were cross-linked with psoralen (*10*), enriched in replication intermediates by binding and elution from BND cellulose (benzoylated naphthoylated DEAE cellulose), and analyzed by electron microscopy under nondenaturing and denaturing conditions.

Wild-type cells exhibit replicating bubbles with normal forks (Fig. 1A). Conversely, ~75% of the replication intermediates in *rad53* cells contained large single-stranded regions at the forks (Fig. 1, B to D). We frequently found bubbles with gaps in both leading or both lagging strands (Fig. 1B). In 40% of the replication intermediates, one parental strand is replicated, whereas the complementary parental strand remains single-stranded (hemi-replicated molecules; Fig. 1, C and F; table S1). We also found adjacent bubbles (Fig. 1D), likely due to firing of pseudo or dormant (*11*, *12*) origins of replication. Again, most of the bubbles were hemi-replicated (Fig. 1D). In wild-type cells bubble size increases with time (Table 1), whereas the single-stranded regions remain constant [~320 nucleotides (nt), Fig. 1E, table S1]. In *rad53* cells, bubbles exhibit a marginal increase in size (Table 1), whereas the extent of the single-stranded regions roughly doubles (Fig. 1E, table S1). In wild-type cells, the ratio between bubbles and

[1]Institute of Cell Biology, ETH Hönggerberg, CH-8093 Zürich, Switzerland. [2]Istituto F.I.R.C. di Oncologia Molecolare, Via Adamello 16, 20141, Milano, Italy, and Dipartimento di Genetica e di Biologia dei Microrganismi, Università degli Studi di Milano, Via Celoria 26, 20133, Milano, Italy.

*These authors contributed equally to this work.
†To whom correspondence should be addressed. E-mail: foiani@ifom-firc.it

26 July 2002

Science

Vol. 297 No. 5581
Pages 465–724 $9

Genome Instability

AMERICAN ASSOCIATION FOR THE ADVANCEMENT OF SCIENCE

Y-shaped forks remains constant throughout the treatment, whereas in *rad53* cells the fraction of Y molecules increases (Table 1). We found that *rad53* cells specifically accumulate hemi-replicated Y molecules, which probably result from breakage of hemi-replicated bubbles (25% at 2 hours in *rad53* cells compared with 1.9% in wild-type cells). We conclude that hydroxyurea-treated wild-type cells exhibit normal replication forks that can still sustain very slow DNA synthesis (~50 bp min^{-1}). Conversely, replication forks in hydroxyurea-treated *rad53* cells are blocked. The accumulation of ssDNA regions may reflect a problem in synthesizing DNA, perhaps because of a defect in lagging- or leading-strand synthesis. Alternatively, these abnormal structures may result from nucleolytic processing of newly synthesized chains.

We found that untreated wild-type cells accumulate short gaps of ~220 nt at the forks (Fig. 1E, table S1). These gaps may represent the regions engaged by the replisome during replication; their size increases by ~100 nt in the presence of hydroxyurea (Fig. 1E, table S1), probably because one newly synthesized strand is preferentially elongated more than the other, leading to the asymmetric accumulation of ssDNA. Thus, the ssDNA might represent the checkpoint signal that leads to Mec1 activation and Rad53 phosphorylation, and indeed, ssDNA has been implicated in checkpoint activation (*13*, *14*). Each fired origin in the presence of hydroxyurea would accumulate ~200 nt of additional ssDNA, which suggests that a critical number of origins would have to be fired for checkpoint activation, consistent with evidence that a specific threshold of ssDNA is required (*15*). This signal could be amplified substantially in hydroxyurea-treated *rad53* cells. Accordingly, the hydroxyurea treatment in *rad53* cells causes irreversible Mec1 activation and in trans phosphorylation of the mutant Rad53 protein (*4*).

Under denaturing conditions (*10*), nucleosome-packed DNA appears as rows of single-stranded bubbles of ~150 nt connected by short duplex regions that correspond to the linkers between adjacent nucleosomes where psoralen cross-links are formed [Fig. 2 (*10*)]; this assay corroborates the finding that *rad53* cells accumulate single-stranded gaps at the forks and hemi-replicated intermediates. We found that newly replicated DNA and the unreplicated sections at the forks in wild-type and *rad53* cells are composed of the typical single-stranded bubbles arising from chromatin DNA packaged into nucleosomes [Fig. 2, A to D (*10*)]. The bubble size, corresponding to mononucleosomes of newly replicated and parental chromatin, is within the range for correctly assembled chromatin [(*10*), table S2], suggesting that, in *rad53* cells, chromatin organization at the forks is normal.

rad53 cells treated with hydroxyurea accumulate DNA structures that, by two-dimensional gel analysis, resemble X-shaped molecules (*4*). Several reversed forks (*16*) were identified in hydroxyurea-treated *rad53* cells (Fig. 3, table S3). Because chromatin DNA was stabilized by psoralen cross-linking in vivo, we conclude that in *rad53* cells certain replication intermediates are stably converted into reversed forks. Most of the reversed forks exhibit a fourth double-stranded regressed arm (Fig. 3, A to C); in a few cases, this fourth arm can be visualized as a single-stranded free tail (Fig. 3D) or as a partially double-stranded tail with a single-stranded terminal (Fig. 3E). These regressed single-stranded arms could arise from forks in which one of the parental strand was not completely replicated (*17*) or, alternatively, from nucleolytic processing of double-stranded reversed forks, eventually producing hemi-replicated molecules (Fig. 4C). We also found bubbles with both forks reversed (Fig. 3F).

Table 1. Classes and size of replication intermediates in the presence of hydroxyurea (HU). Data related to Figs. 1 and 2. Total number of analyzed RIs is in parentheses. wt, wild type.

Cells and treatment	Bubbles (%)	Y-shaped molecules + broken bubbles (%)	RI (*n*)	Size of replicating bubbles (bp)	RI (*n*)
wt + HU 0.5 hours	71.3	28.7	(*230*)	3025 ± 1732	(*149*)
wt + HU 1 hours	74.5	25.5	(*141*)	4227 ± 1807	(*100*)
wt + HU 2 hours	76	24	(*104*)	7484 ± 4155	(*76*)
rad53 + HU 0.5 hours	70.8	29.2	(*181*)	2099 ± 1681	(*106*)
rad53 + HU 1 hours	77.5	22.5	(*165*)	2747 ± 1355	(*87*)
rad53 + HU 2 hours	45.8	54.2	(*144*)	3116 ± 1991	(*56*)

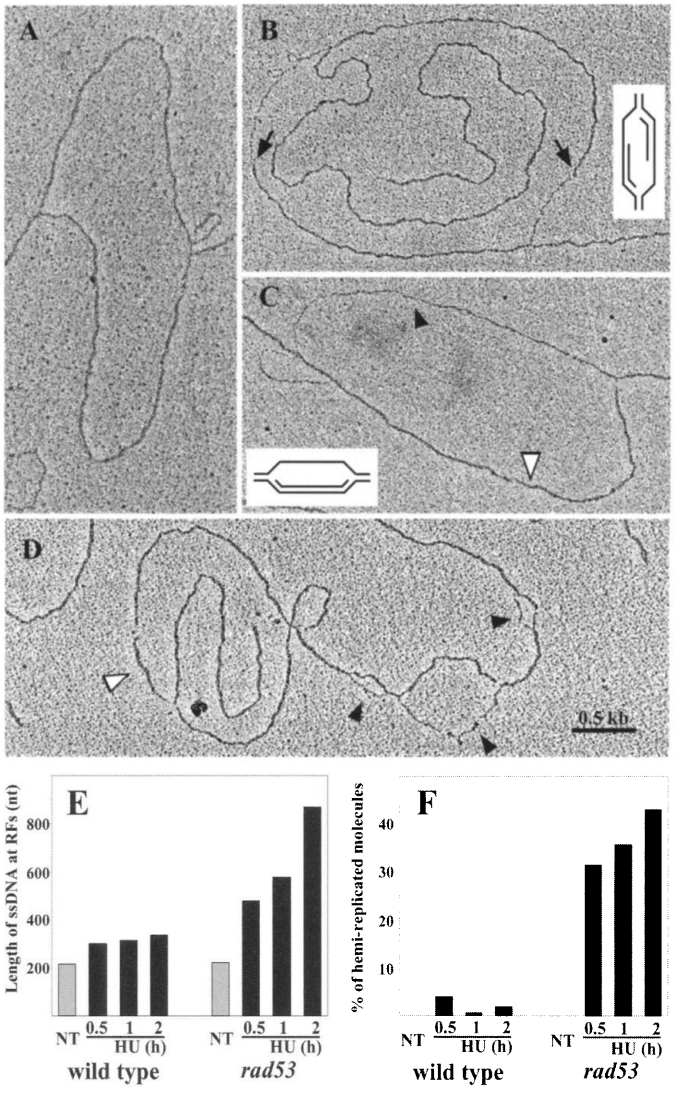

Fig. 1. Representative RIs isolated from in vivo psoralen cross-linked chromatin. Electron micrographs of replicating bubbles from wild-type (**A**) or *rad53* (**B** and **C**) cells (*27*). The transition point from dsDNA to ssDNA is indicated by arrows (B). Black arrowheads indicate the single-stranded arms of the hemi-replicated bubbles; white arrowheads indicate the replicated strands (C and **D**). Graphic representation of the data in table S2 for hydroxyurea (HU)-treated or untreated (no treatment, NT) wild-type and *rad53* cells for the number of hours (h) shown (**E** and **F**).

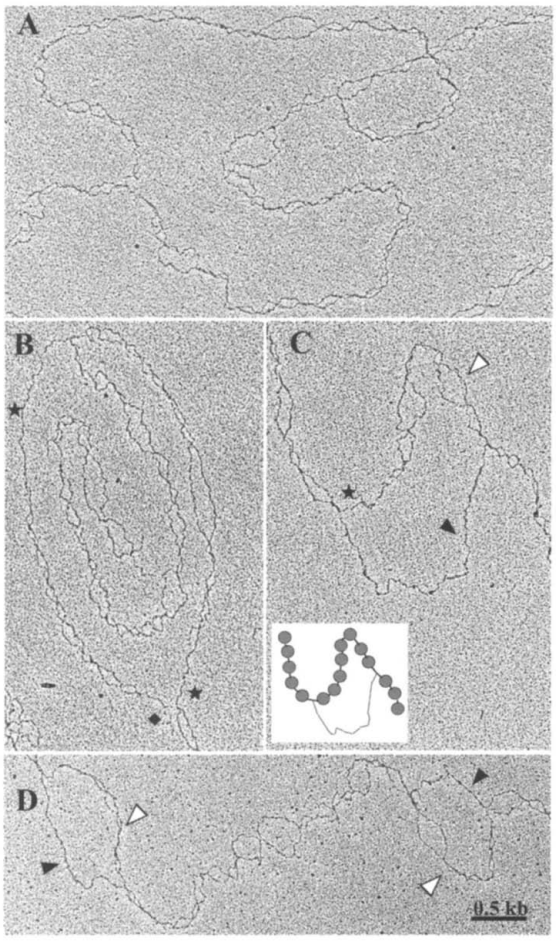

Fig. 2. Representative RIs purified as in Fig. 1 and analyzed under denaturing conditions. Replicating molecules from wild-type (**A**) and *rad53* cells (**B** to **D**). The density of single-stranded bubbles representing nucleosomes (*10*) is similar in parental and daughter strands (table S2). Asterisks indicate large gaps at the forks (B and C). In (B), a fork containing single-stranded regions in both arms is visualized (asterisk and diamond). Black arrowheads indicate the single-stranded arms of the hemi-replicated bubbles; white arrowheads indicate the replicated strands (C and D). (A to D) Replicated arms are organized in single-stranded bubbles reflecting nucleosome assembly [see drawing in (C)].

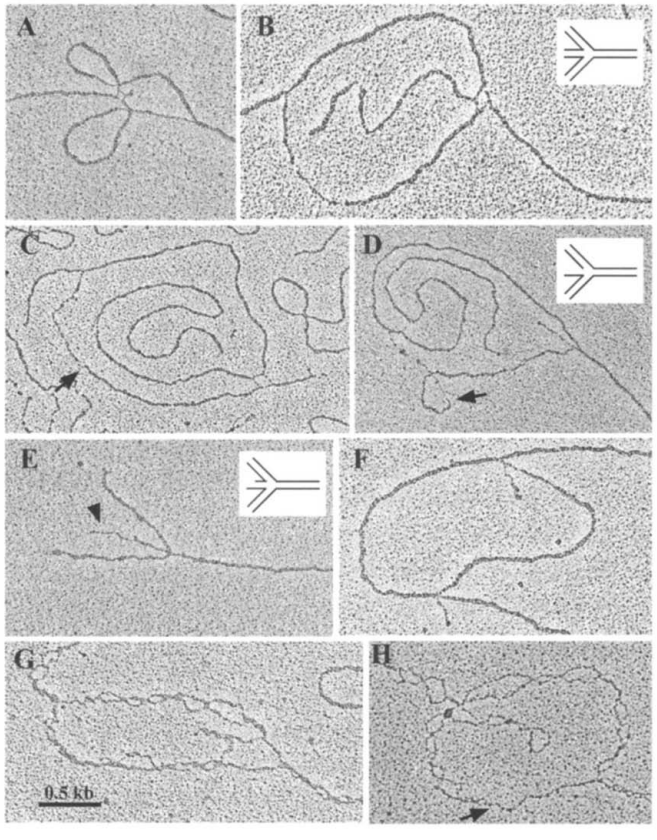

Fig. 3. RIs containing four-way junctions from HU-treated *rad53* cells. In most of the Holliday junctions formed at the replication forks, the four single strands involved in the branch point are visualized [(A), (B), (C), (G)]. (**A** to **F**) Samples were prepared under nondenaturing conditions. Arrows indicate single-stranded regions [(C) and (D)]. (**G**) and (**H**) Samples were prepared under denaturing conditions. In (H), the fourth arm is organized in single-stranded bubbles characteristic of nucleosomal DNA.

The regressed arm of the Holliday junction at the forks is organized in single-stranded bubbles resembling nucleosomal organization (Fig. 3H). In this view, the disassembly and assembly of nucleosomes during the formation of the regressed strands would mimic the dynamics of nucleosome formation during normal fork elongation (*10*).

The finding that the hydroxyurea treatment per se is not sufficient to cause accumulation of reversed forks in wild-type cells suggests that they are pathological structures, rather than physiological intermediates resulting from stalled replication forks. Accordingly, previous attempts to visualize reversed forks in wild-type cells experiencing replication pausing have failed (*18*). However, we cannot exclude that in hydroxyurea-treated wild-type cells reversed forks are too transient or too short to be detected by our assay.

In conclusion, two classes of abnormal DNA structures accumulate in hydroxyurea-treated *rad53* cells: replication intermediates with long single-stranded regions and reversed forks. The accumulation of hemi-replicated molecules could result from a defect in coordinating replication of leading and lagging-strand. This is supported by the following observations: (i) phosphorylation of lagging-strand polymerase and replication factor A depends on a functional Rad53 pathway (*6*, *19*). (ii) Certain primase mutants mimic *rad53* checkpoint defects (*20*). (iii) Primase mutants, despite exhibiting an active checkpoint (*20*), accumulate single-stranded regions at the forks (~900 nt), and 40% of these intermediates are hemi-replicated (Fig. 4, A and B). This last finding suggests that in hydroxyurea-treated *rad53* cells the DNA primase-dependent initiation and elongation steps are limiting (Fig. 4C).

Replication intermediates represent perfect substrates for recombination enzymes when replication is defective (*21*). Hence, in *rad53* cells, stalled forks could be enzymatically processed, originating ssDNA intermediates, reversed forks, and breaks (Fig. 4C). This is supported by the findings that Rad53 modulates phosphorylation of several recombination enzymes (*22*, *23*) and that recombination proteins have been suggested to process the DNA structures accumulating in checkpoint mutants (*24*, *25*). We propose that the replication checkpoint prevents genomic instability and cancer by coordinating DNA replication and recombination.

References and Notes

1. K. Myung, A. Datta, R. D. Kolodner, *Cell* **104**, 397 (2002)
2. T. Weinert, *Cancer Surv.* **29**, 109 (1997).
3. N. F. Lowndes, J. R. Murguia, *Curr. Opin. Genet. Dev.* **10**, 17 (2000).
4. M. Lopes *et al.*, *Nature* **412**, 557 (2001)
5. J. A. Tercero, J. F. X. Diffley, *Nature* **412**, 553 (2001).
6. A. Pellicioli *et al.*, *EMBO J.* **18**, 6561 (1999)

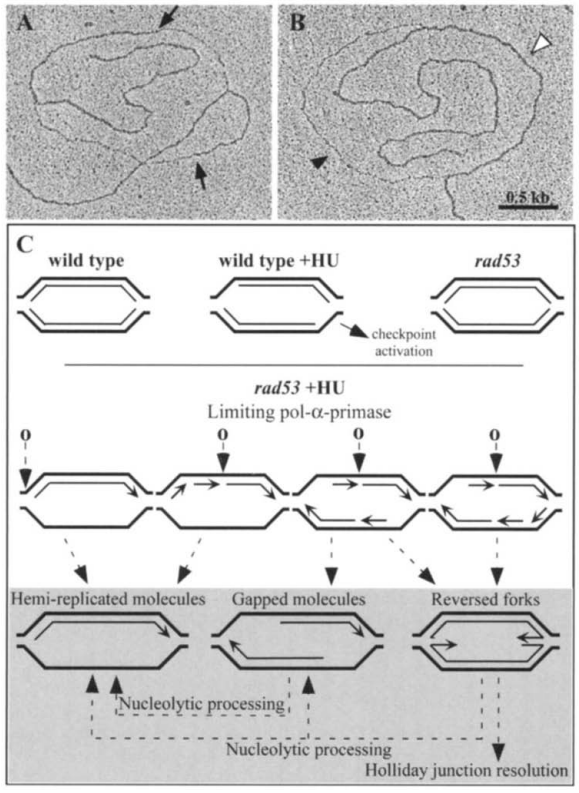

Fig. 4. DNA primase mutants accumulate hemi-replicated intermediates. Representative replicating bubbles from *pri1-M4* mutant cells (**A** and **B**) (*27*). The molecule in (A) is partially single-stranded. Arrows indicate the transition points from dsDNA to ssDNA. In (B), the white arrowhead indicates the replicated arm of a hemi-replicated bubble; the black arrowhead indicates the unreplicated strand. (**C**) Schematic representation of RIs in wild-type and *rad53* cells treated with HU or not treated. In HU-treated wild-type cells, the accumulation of short single-stranded regions likely causes checkpoint activation. In HU-treated *rad53* cells, abnormal replication intermediates, likely caused by a defect in the DNA polymerase α-primase complex, are converted into the aberrant structures represented in the gray panel. O, replication origin.

7. H. D. Lindsay *et al.*, *Genes Dev.* **12**, 382 (1998).
8. B. A. Desany, A. A. Alcasabas, J. B. Bachant, S. J. Elledge, *Genes Dev.* **12**, 2956 (1998).
9. R. Lucchini, J. M. Sogo, *Nature* **374**, 276 (1995).
10. R. Gasser, T. Koller, J. M. Sogo, *J. Mol. Biol.* **258**, 224 (1996).
11. C. Santocanale, J. F. X. Diffley, *Nature* **395**, 615 (1998).
12. K. Shirahige *et al.*, *Nature* **395**, 618 (1998).
13. B. Garvik, M. Carson, L. Hartwell, *Mol. Cell. Biol.* **11**, 6128 (1995).
14. S. E. Lee *et al.*, *Cell* **94**, 399 (1998).
15. M. B. Vaze, A. Pellicioli, M. Foiani, J. Haber, unpublished data.
16. R. B. Inmann, *Biochim. Biophys. Acta* **783**, 205 (1984).
17. M. R. Singleton, S. Scaife, D. B. Wigley, *Cell* **107**, 79 (2001).
18. M. Gruber, R. E. Wellinger, J. M. Sogo, *Mol. Cell. Biol.* **20**, 5777 (2000)
19. G. Brush, D. M. Morrow, P. Heiter, T. J. Kelly, *Proc. Natl. Acad. Sci. U.S.A.* **93**, 15075 (1996).
20. F. Marini *et al.*, *EMBO J.* **16**, 639 (1997).
21. M. Seigneur, V. Bidnenko, S. D. Ehrlich, B. Michel, *Cell* **95**, 419 (1998).
22. G. Liberi *et al.*, *EMBO J.* **19**, 5027 (2000).
23. V. Bashkirov *et al.*, *Mol. Cell. Biol.* **20**, 4393 (2000).
24. M. N. Boddy, P. Russell, *Curr. Biol.* **11**, 953 (2001)
25. J. E. Haber, W. D. Heyer, *Cell* **107**, 551 (2001).

26. We thank C. Gutierrez, J. Haber, N. Mantei, H. Mayer-Rosa, C. Newlon, P. Plevani, R. Rothstein, D. Sargent, U. Suter, F. Thoma, R. E. Wellinger, and all the members of our laboratories for discussions and support. We thank R. Cha and N. Kleckner for communicating unpublished results. This work was supported by Associazione Italiana per la Ricerca sul Cancro and partially by grants from Telethon-Italy, European Union Grant RTN2-2001-00177 and Schweizerischer Nationalfonds zur Förderung der Wissenschaflichen Forschung. M.L. was a recipient of the short-term EMBO fellowship N.9779.

Supporting Online Material
www.sciencemag.org/cgi/content/full/297/5581/599/DC1
Materials and Methods
Tables S1 to S3

26 February 2002; accepted 28 May 2002

ATR Homolog Mec1 Promotes Fork Progression, Thus Averting Breaks in Replication Slow Zones

Rita S. Cha and Nancy Kleckner*

Budding yeast Mec1, homolog of mammalian ATR, is an essential protein that mediates S-phase checkpoint responses and meiotic recombination. Elimination of Mec1 function leads to genomewide fork stalling followed by chromosome breakage. Breaks do not result from stochastic collapse of stalled forks or other incidental lesions; instead, they occur in specific regions of the genome during a G_2 chromosomal transition. Break regions are found to be genetically encoded replication slow zones (*RSZs*), a newly discovered yeast chromosomal determinant. Thus, Mec1 has important functions in normal S phase and the genome instability of *mec1* (and, analogously, *ATR*$^{-/-}$) mutants stems from defects in these basic roles.

Proteins of the ATR/ATM family (mammalian ATR and ATM, *Drosophila* mei-41, *Schizosaccharomyces pombe* rad3$^+$, and budding yeast Mec1 and Tel1) are chromosome-bound signal transduction proteins involved in DNA replication, repair, and recombination (*1*, *2*). These proteins are best understood as mediators of checkpoint responses: They sense the presence of damage or aberrations in the genome and transmit appropriate signals that trigger cell cycle arrest and coordinate repair. However, in addition, mutations in these genes confer defects during the unchallenged life of the cell. Many of these defects are also typically associated with exposure to exogenous genotoxic agents—for example, occurrence of double-strand breaks (DSBs), genome instability, and inviability. This relationship has led to a model in which potentially lethal lesions arise spontaneously during normal cellular life, with Mec1 and its homologs being required for processing of such incidental lesions (*1*, *2*). Mec1 is also involved in up-regulation of deoxynucleotide triphosphate (dNTP) synthesis through its essential downstream target Rad53, which in turn inactivates Sml1, an inhibitor of Rnr1 (*3*). Inability to up-regulate dNTP synthesis is proposed to contribute to the *mec1* phenotypes by inducing "replication stress"—that is, stalled forks that undergo irreversible collapse and/or are processed by recombination proteins into DSBs (*2*, *4*).

Alternatively, during unchallenged life, ATM/ATR/Mec1 could coordinate and promote basic chromosomal events, with the observed mutant phenotypes arising from defects in these fundamental processes, regardless of any failure to respond to incidental lesions. This notion is supported by the fact that Mec1 and its homologs are required for processes that probably occur independently of incidental damages or accidental fork stalling: the G_1 to S transition (*5*), regulation of crossover position and partner choice during meiotic recombination (*6*, *7*), and establishment of late origin firing (*8*).

Department of Molecular and Cellular Biology, Harvard University, Cambridge, MA 02138, USA.

*To whom correspondence should be addressed. E-mail: kleckner@fas.harvard.edu.